OBES SURG
DOI 10.1007/s11695-015-1612-z

ORIGINAL CONTRIBUTIONS

Sleeve Gastrectomy Reduces Hepatic Steatosis by Improving the Coordinated Regulation of Aquaglyceroporins in Adipose Tissue and Liver in Obese Rats

Leire Méndez-Giménez · Sara Becerril · Rafael Moncada · Víctor Valentí · Beatriz Ramírez · Andoni Lancha · Javier Gurbindo · Inmaculada Balaguer · Javier A. Cienfuegos · Victoria Catalán · Secundino Fernández · Javier Gómez-Ambrosi · Amaia Rodríguez · Gema Frühbeck

Abstract
Background Glycerol constitutes an important metabolite for the control of lipid accumulation and glucose homeostasis. Our aim was to investigate the potential role of aquaglyceroporins, which are glycerol channels mediating glycerol efflux in adipocytes (AQP3 and AQP7) and glycerol influx (AQP9) in hepatocytes, in the improvement of adiposity and hepatic steatosis after sleeve gastrectomy in an experimental model of diet-induced obesity (DIO).
Methods Male Wistar DIO rats (n=161) were subjected to surgical (sham operation and sleeve gastrectomy) or dietary interventions [fed ad libitum a normal diet (ND) or a high-fat diet (HFD) or pair-fed to the amount of food eaten by sleeve-gastrectomized animals]. The tissue distribution and expression of AQPs in biopsies of epididymal (EWAT) and subcutaneous (SCWAT) white adipose tissue and liver were analyzed by real-time PCR, Western blot, and immunohistochemistry.
Results Four weeks after surgery, DIO rats undergoing sleeve gastrectomy showed a reduction in body weight, whole-body adiposity, and hepatic steatosis. DIO was associated with a tendency towards an increase in EWAT AQP3 and SCWAT AQP7 and a decrease in hepatic AQP9. Sleeve gastrectomy downregulated AQP7 in both fat depots and upregulated AQP3 in EWAT, without changing hepatic AQP9. *Aqp7* transcript levels in EWAT and SCWAT were positively associated with adiposity and glycemia, while *Aqp9* mRNA was negatively correlated with markers of hepatic steatosis and insulin resistance.
Conclusion Our results show, for the first time, that sleeve gastrectomy, a widely applied bariatric surgery procedure, restores the coordinated regulation of fat-specific AQP7 and

Electronic supplementary material The online version of this article (doi:10.1007/s11695-015-1612-z) contains supplementary material, which is available to authorized users.

L. Méndez-Giménez · S. Becerril · B. Ramírez · A. Lancha · J. Gurbindo · I. Balaguer · V. Catalán · J. Gómez-Ambrosi · A. Rodríguez · G. Frühbeck
Metabolic Research Laboratory, Clínica Universidad de Navarra, Pamplona, Spain

R. Moncada
Department of Anesthesiology, Clínica Universidad de Navarra, Pamplona, Spain

V. Valentí · J. A. Cienfuegos
Department of Surgery, Clínica Universidad de Navarra, Pamplona, Spain

S. Fernández
Department of Otorhinolaryngology, Clínica Universidad de Navarra, Pamplona, Spain

G. Frühbeck (✉)
Department of Endocrinology and Nutrition, Clínica Universidad de Navarra, Avda. Pío XII, 36, 31008 Pamplona, Spain
e-mail: gfruhbeck@unav.es

L. Méndez-Giménez · S. Becerril · R. Moncada · V. Valentí · B. Ramírez · J. A. Cienfuegos · V. Catalán · J. Gómez-Ambrosi · A. Rodríguez · G. Frühbeck
Obesity and Adipobiology Group, Instituto de Investigación Sanitaria de Navarra (IDISNA), Pamplona, Spain

L. Méndez-Giménez · S. Becerril · R. Moncada · V. Valentí · B. Ramírez · J. A. Cienfuegos · V. Catalán · J. Gómez-Ambrosi · A. Rodríguez · G. Frühbeck
CIBER Fisiopatología de la Obesidad y Nutrición, Instituto de Salud Carlos III, Pamplona, Spain

Published online: 04 March 2015

liver-specific AQP9, thereby improving whole-body adiposity and hepatic steatosis.

Keywords Aquaporins · Glycerol · Bariatric surgery · Obesity · Fatty liver

Abbreviations

Adipo-IR	Adipocyte insulin resistance index
AQP	Aquaporin
CSA	Cell surface area
DIO	Diet-induced obesity
EWAT	Epididymal white adipose tissue
FFA	Free fatty acids
GK	Glycerol kinase
HFD	High-fat diet
HOMA	Homeostasis model assessment
NAFLD	Non-alcoholic fatty liver disease
ND	Normal diet
PPARγ	Peroxisome proliferator-activator receptor γ
QUICKI	Quantitative insulin sensitivity check index
RT	Room temperature
SCWAT	Subcutaneous white adipose tissue
SREBF1	Sterol regulatory element-binding factor 1
TG	Triacylglycerol

Introduction

Aquaporins are channel-forming integral membrane proteins that facilitate the movement of water across cell membranes [1]. To date, 13 aquaporins have been identified in mammalian tissues (AQP0-12), which can be divided into three subgroups according to their permeability and structure, namely aquaporins, aquaglyceroporins, and superaquaporins [1, 2]. Aquaglyceroporins (AQP3, 7, 9, and 10) encompass a subfamily of aquaporins that facilitate the movement of water and other small solutes, such as glycerol, across the plasma membranes [3, 4]. In this sense, glycerol constitutes a key metabolite as a direct source of glycerol-3-phosphate for the synthesis of triacylglycerols (TG) and an important substrate for hepatic gluconeogenesis during fasting [5]. Adipose tissue is the major source of circulating glycerol. AQP7 represents the main gateway for the delivery of fat-derived glycerol into the bloodstream [6, 7], although other glycerol channels, such as AQP3, AQP9, AQP10, and the more recently identified AQP11, also contribute to glycerol release from adipocytes [8–10].

Plasma glycerol is introduced into hepatocytes by the liver-specific AQP9, where it is transformed into glycerol-3-phosphate by glycerol kinase (GK) for de novo synthesis of glucose and TG [11, 12]. Functional studies in transgenic mice lacking aquaglyceroporins have revealed their relevance in the onset of obesity and insulin resistance. In this regard, *Aqp3* deletion is associated with nephrogenic diabetes insipidus [13], *Aqp7*-knockout mice develop adult-onset obesity [6, 7], and *Aqp9* deficiency leads to a defective hepatic glycerol metabolism, confirming that AQP9 is the primary route for hepatocyte glycerol uptake for glycerol gluconeogenesis in mice [12, 14]. Interestingly, the murine *Aqp10* gene is a pseudogene [15].

Obesity is associated with an altered expression of aquaglyceroporins in adipose tissue and liver [8, 16–20]. Dysregulation of aquaglyceroporins in adipose tissue shows fat depot-specific differences. Visceral fat exhibits higher expression of AQP3 and AQP7, which might reflect an overall increase in lipolytic rate and glycerol release in this fat depot, while the repression of AQP7 in subcutaneous fat points to the promotion of an intracellular glycerol accumulation and a progressive adipocyte hypertrophy [8, 18]. On the other hand, obesity-associated metabolic derangements, such as type 2 diabetes or non-alcoholic fatty liver disease are associated with a downregulation of hepatic AQP9, suggesting a compensatory mechanism whereby the liver counteracts further TG accumulation within its parenchyma as well as reduces hepatic gluconeogenesis [8, 18, 19]. In this regard, a recent study reported that *Aqp9* knockdown with small interference RNA prevents steatosis in an oleic acid-treated LO2 immortal liver cell line, supporting a key role for AQP9 in the onset of fatty liver [21]. Thus, the coordinated regulation of aquaglyceroporin expression in the adipose tissue and the liver is extremely relevant to maintain the control of adipose and hepatic TG accumulation as well as for glucose homeostasis [8, 11].

Sleeve gastrectomy constitutes a widely applied bariatric surgery procedure to induce weight loss in obese patients that leaves a lesser curvature tube after excising the fundus and greater curvature portion of the stomach [22]. This bariatric surgical technique induces an effective and sustained weight loss in humans [22, 23] as well as in experimental models of genetic and diet-induced obesity (DIO) [24–26]. However, the molecular mechanisms underlying the improvement of adiposity after sleeve gastrectomy are poorly understood. Therefore, the aim of the present study was to analyze the potential participation of aquaglyceroporins in the improvement of adiposity and hepatic steatosis after sleeve gastrectomy in an experimental model of DIO, which leads to non-alcoholic fatty liver disease (NAFLD). Moreover, it is well known that peroxisome proliferator-activated receptor γ (PPARγ) and sterol regulatory element-binding transcription factor 1 (SREBF1) are key elements in the control of adipose-specific genes [27] and that the *AQP7* gene exhibits response elements for these transcription factors in its promoter [28]. Thus, we further studied the transcription of the *Pparg* and *Srebf1* genes in white adipose tissue and liver as well as their plausible association with the gene expression of *Aqp7* and the other aquaglyceroporins in these metabolic tissues.

Material and Methods

Experimental Animals and Study Design

Four-week-old male Wistar rats (n=161) (breeding house of the University of Navarra) were housed in individual cages in a room with controlled temperature (22±2 °C), ventilation (at least 15 complete air changes), 12:12-h light–dark cycle (lights on at 8:00 am), and relative humidity (50±10 %) under pathogen-free conditions. Animals were fed ad libitum during 4 months with either a normal diet (ND) (n=22) (12.1 kJ: 4 % fat, 82 % carbohydrate, and 14 % protein, diet 2014S, Harlan, Teklad Global Diets, Harlan Laboratories Inc., Barcelona, Spain) or a high-fat diet (HFD) (n=139) (23.0 kJ/g: 59 % fat, 27 % carbohydrate, and 14 % protein, diet F3282; Bio-Serv, Frenchtown, NJ, USA) [29]. Body weight and food intake were registered weekly to monitor the progression of the DIO rats that reached a mean body weight of 630±15 g after 4 months on the HFD.

DIO rats were randomized into weight-matched groups to be submitted either to the sleeve gastrectomy (n=37) or a sham operation (n=41). Anesthesia and sleeve gastrectomy were performed according to previously described methodology [25, 26, 30]. Briefly, for the sleeve gastrectomy, a laparotomy incision was made in the abdominal wall and the stomach was isolated outside the abdominal cavity. Loose gastric connections to the spleen and liver were released along the greater curvature, and the great omentum was ligated and divided down to the level of the pylorus. About 60–70 % of the forestomach and glandular stomach was excised out using an automatic stapler (AutoSuture TA DST Series, Tyco Healthcare group LP, Norwalk, CT, USA) with a TA30V3L load, leaving a tubular gastric remnant in continuity with the esophagus upwards and the pylorus and duodenum downwards. The sham surgery comprised the same laparotomic incision as well as handling of the stomach except for the gastrectomy. Following the surgical interventions [sham operation (n=24) or sleeve gastrectomy (n=22)], a group of DIO animals continued to be fed ad libitum a HFD, while another group of DIO rats was switched to a ND ad libitum [sham operation (n=17) or sleeve gastrectomy (n=15)]. In order to discriminate the effects of a reduced food intake following the bariatric surgery, two groups of DIO rats were pair-fed to the amount of food eaten by the animals undergoing the sleeve gastrectomy switched to either the ND or the HFD [pair-fed ND (n=17) or pair-fed HFD (n=23)]. Four weeks after the surgical and dietary interventions, rats were killed by decapitation after an 8-h fasting period. The liver, epididymal (EWAT), and subcutaneous (SCWAT) white adipose tissues were carefully dissected out, weighed, frozen in liquid nitrogen, and stored at −80 °C until processed for each study. A small portion of the diverse tissues was fixed in 4 % paraformaldehyde for histological analyses. Blood samples were immediately collected and sera were obtained by cold centrifugation (4 °C) at 700g for 15 min.

All applicable institutional and/or national guidelines for the care and use of animals were followed. All experimental procedures conformed to the European Guidelines for the care and use of Laboratory Animals (directive 2010/63/EU) and were approved by the Ethical Committee for Animal Experimentation of the University of Navarra (049/10).

Blood and Tissue Analysis

Serum glucose was determined by an automatic glucose sensor (Ascencia Elite, Bayer, Barcelona, Spain). Serum concentrations of free fatty acids (FFA), TG, and total cholesterol were measured by enzymatic methods using commercially available kits (Infinity™, Thermo Electron Corporation, Melbourne, Australia). Serum glycerol levels were analyzed using a free glycerol determination kit, a quantitative enzymatic determination assay (Sigma, St. Louis, MO, USA); intra- and interassay coefficients of variation were 3.3 and 4.2 %, respectively. Intrahepatic TG was determined by enzymatic methods, as previously described [8]. Insulin and leptin were determined by ELISA (Crystal Chem, Inc., Chicago, IL, USA) [31, 32]. Intra- and interassay coefficients of variation for measurements of insulin and leptin were 3.5 and 6.3 %, respectively, for the former, and 5.4 and 6.9 %, for the latter. Insulin resistance was calculated using the homeostasis model assessment (HOMA), calculated with the formula: fasting insulin (μU/mL) × fasting glucose (mmol/L)/22.5). An indirect measure of insulin sensitivity was calculated using the quantitative insulin sensitivity check index (QUICKI) as follows: 1/[log(fasting insulin [μU/mL])+log(fasting glucose [mg/dL]). The adipocyte insulin resistance (Adipo-IR) index, as a surrogate of adipocyte dysfunction, was calculated as fasting FFA (mmol/L) × fasting insulin (pmol/L) [20]. Total ghrelin levels were also assessed using a rat/mouse total ghrelin ELISA Kit (#EZRGRT-91 K, Millipore, Billerica, MA, USA). Intra- and interassay coefficients of variation for measurements of total ghrelin were 0.8 and 2.8 %, respectively.

RNA Isolation and Real-Time PCR

RNA isolation and purification were performed as earlier described [33]. Transcript levels of *Aqp3*, *Aqp7*, *Aqp9*, *Pparg*, and *Srebf1* were quantified by real-time PCR (7300 Real-Time PCR System, Applied Biosystems, Foster City, CA, USA). Primers and probes (Supplemental Table 1) were designed using the software Primer Express 2.0 (Applied Biosystems) and acquired from Genosys (Sigma). Primers or TaqMan® probes encompassing fragments of the areas from the extremes of two exons were designed to ensure the detection of the corresponding transcript avoiding genomic DNA amplification. The cDNA was amplified at the following

conditions: 95 °C for 10 min, followed by 45 cycles of 15 s at 95 °C and 1 min at 59 °C, using the TaqMan® Universal PCR Master Mix (Applied Biosystems). The primer and probes concentrations were 300 and 200 nmol/L, respectively. All results were normalized for the expression of *18S* rRNA (Applied Biosystems), and relative quantification was calculated as fold expression over the calibrator sample [18]. All samples were run in triplicate and the average values were calculated.

Western Blot Studies

Tissues and cells were harvested and homogenized in ice-cold lysis buffer (0.1 % SDS, 1 % Triton X-100, 5 mmol/L EDTA·$2H_2O$, 1 mol/L Tris–HCl, 150 mmol/L NaCl, 1 % sodium deoxycholate, pH 7.40) complemented with a protease inhibitor cocktail (Complete™ Mini-EDTA free, Roche, Mannheim Germany). Lysates were centrifuged at 12,000 *g* at 4 °C for 15 min to remove nuclei and unruptured cells. Total protein concentrations were determined by the Bradford assay, using bovine serum albumin (BSA) (Sigma) as standard. Thirty micrograms of total protein were diluted in loading buffer 4× (20 % β-mercaptoethanol, 40 mmol/L dithiothreitol, 8 % SDS, 40 % glycerol, 0.016 % bromophenol blue, 200 mmol/L Tris–HCl, pH 6.80) and heated for 10 min at 100 °C. Samples were run out in Mini-PROTEAN® TGX™ precast gels (Bio-Rad Laboratories, Inc., Hercules, CA, USA), subsequently transferred to PVDF membranes (Bio-Rad) and blocked in Tris-buffered saline (10 mmol/L Tris–HCl, 150 mmol/L NaCl, pH 8.00) with 0.05 % Tween 20 (TBS-T) containing 5 % non-fat dry milk for 1 h at room temperature (RT). Membranes were then incubated overnight at 4 °C with goat polyclonal anti-AQP3, rabbit polyclonal anti-AQP7, goat polyclonal anti-AQP9 (Santa Cruz Biotechnology, Inc., Santa Cruz, CA, USA) antibodies (diluted 1:5000 for AQP3 and 1:1000 for AQP7 and AQP9 in blocking solution) or murine monoclonal anti-β-actin (Sigma) (diluted 1:5000 in blocking solution). The antigen-antibody complexes were visualized using horseradish peroxidase (HRP)-conjugated anti-goat, anti-rabbit, or anti-mouse IgG antibodies (diluted 1:5000 in blocking solution) and the enhanced chemiluminescence ECL Plus detection system (Amersham Biosciences, Buckinghamshire, UK). The intensity of the bands was determined by densitometric analysis with the Gel Doc™ gel documentation system and Quantity One 4.5.0 software (Bio-Rad) and normalized with β-actin density values. All assays were performed in duplicate.

Histological Analyses

The immunodetection of AQP3 and AQP7 in histological sections of EWAT as well as AQP9 in liver was performed by the indirect immunoperoxidase method, as previously described [8, 20]. Sections of formalin-fixed paraffin-embedded adipose tissue (6 μm) and liver (4 μm) were dewaxed in xylene, rehydrated in decreasing concentrations of ethanol, and treated with 3 % H_2O_2 (Sigma) in absolute methanol for 10 min at RT to quench endogenous peroxidase activity. Slides were blocked during 60 min with 1 % murine serum (Sigma) diluted in Tris-buffer saline (TBS) (50 mmol/L Tris, 0.5 mol/L NaCl, pH 7.36) to prevent non-specific absorption. Sections were incubated overnight at 4 °C with goat polyclonal anti-AQP3, rabbit anti-AQP7 or rabbit polyclonal anti-AQP9 (Alpha Diagnostic International, San Antonio, TX, USA) antibodies diluted 1:100 in TBS. After washing three times with TBS (5 min each), slides were incubated with HRP-conjugated anti-goat IgG (Zymed, San Francisco, CA, USA) or DAKO Real™ EnVision™ anti-rabbit/mouse (K5007; Dako, Golstrup, Denmark) for 1 h at RT. The peroxidase reaction was visualized using a 0.5 mg/mL diaminobenzidine (DAB)/0.03 % H_2O_2 solution diluted in 50 mmol/L Tris–HCl, pH 7.36, and Harris hematoxylin solution (Sigma) as counterstaining. Negative control slides without primary antibody were included to assess non-specific staining.

The adipocyte cell surface area (CSA) was measured as previously described [34]. Briefly, biopsies of EWAT were fixed in 4 % formaldehyde, embedded in paraffin, cut into sections of 6 μm and stained with hematoxylin-eosin. Images of three fields per section from each animal were captured with the 20× objective, and the adipocyte CSA from, at least, 100 cells/section was measured using the software AxioVision Release 4.6.3 (Zeiss, Göttingen, Germany).

Statistical Analysis

Data are expressed as the mean±SEM. Statistical differences between mean values were analyzed using two-way ANOVA (diet × surgery) or one-way ANOVA followed by Tukey's *post hoc* test, if an interaction was detected. Pearson correlation coefficients (*r*) were used to analyze the association between variables. The statistical analyses were performed using the SPSS/Windows version 15.0 software (SPSS Inc., Chicago, IL, USA).

Results

Sleeve Gastrectomy Reduces Adiposity and Improves Metabolic Profile

The survival rate of the surgical procedures (both sleeve gastrectomy and sham intervention) was 100 % with no animals being excluded from the study due to complications. As expected, DIO rats showed higher ($P<0.001$) body weight,

whole-body adiposity and adipocyte hypertrophy than their lean counterparts (Fig. 1). Four weeks after the surgical interventions, DIO animals switched to the ND significantly ($P<0.001$) reduced their body weight and total adiposity (Fig. 1a, b). Animals subjected to the sleeve gastrectomy exhibited the highest weight loss reduction ($P<0.001$) as compared to the other intervention groups and in whole-body fat mass even if fed a HFD compared to control DIO rats. In this regard, sleeve-gastrectomized groups showed a decrease ($P<0.05$) in the weight of EWAT and SCWAT compared to sham-operated rats (Fig. 1c). Accordingly, sleeve gastrectomy significantly reduced the size of white adipocytes in EWAT (Fig. 1d, e). Furthermore, rats undergoing the sleeve gastrectomy displayed a higher proportion of small adipocytes and a lower proportion of large adipocytes as determined by the CSA (Fig. 1f). Pair-fed rats also exhibited a reduction in body weight, whole-body adiposity and adipocyte hypertrophy, but to a lesser extent than sleeve-gastrectomized animals, suggesting that changes in body composition after bariatric surgery are beyond food intake reduction.

The general characteristics of the metabolic profile of animals that underwent the surgical and dietary interventions are summarized in Table 1. Sleeve gastrectomy was associated with an improvement in insulin sensitivity, as evidenced by

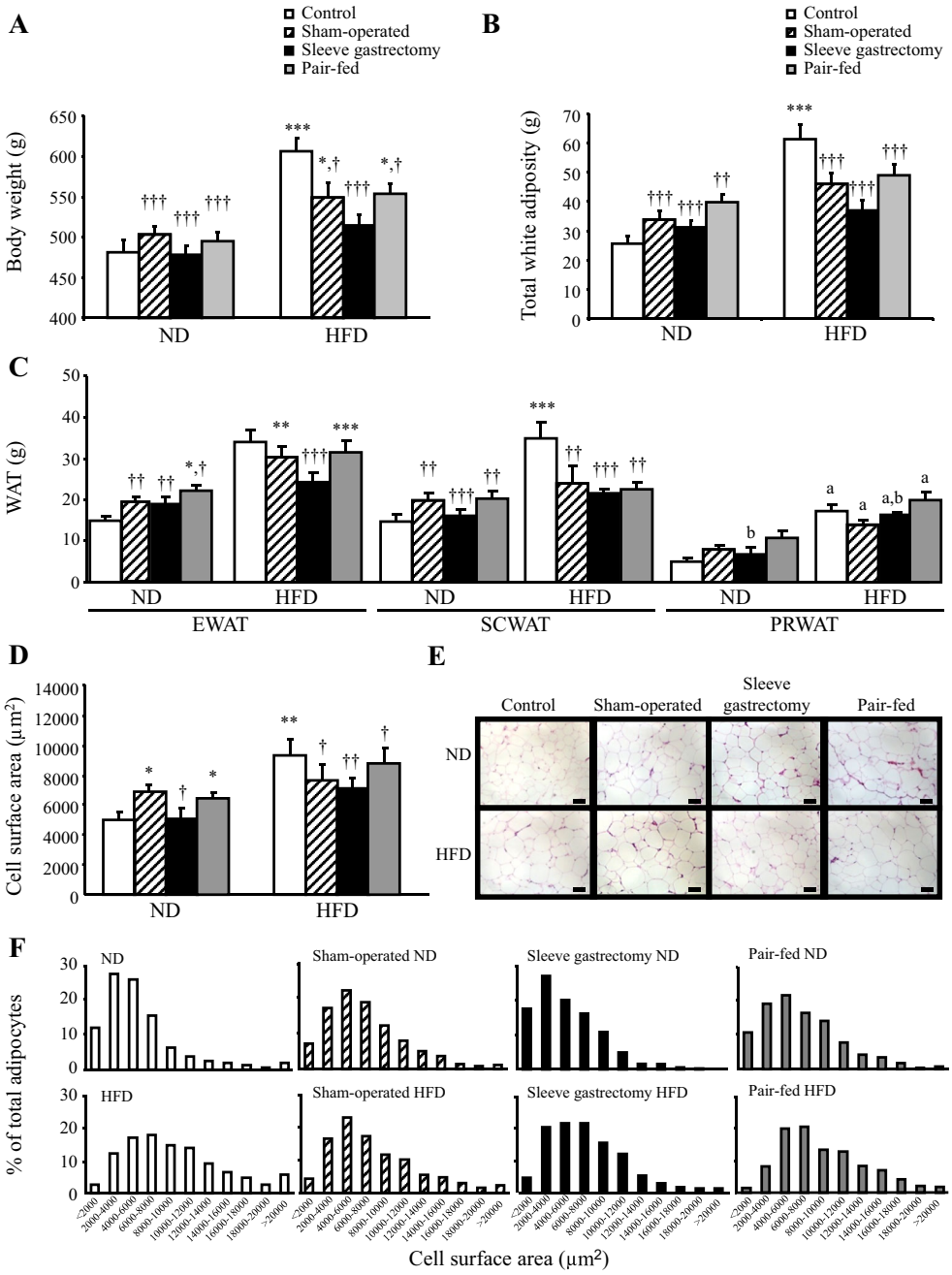

Fig. 1 Impact of sleeve gastrectomy on body weight and whole-body adiposity in diet-induced obese rats. *Bar* graphs show body weight (**a**), total white adiposity (**b**), epididymal (EWAT), subcutaneous (SCWAT) and perirenal (PRWAT) fat content (**c**), as well as cell surface area (CSA) of epididymal white adipocytes (**d**). Representative histological sections of EWAT of all experimental groups (**e**); magnification 100×, *scale bar*= 100 µm. Adipocyte size distribution (**f**) of experimental animals fed either a normal diet (ND) or a high-fat diet (HFD) after surgical interventions. Statistical differences were analyzed by two-way ANOVA or one-way ANOVA followed by Tukey's *post hoc* test, if an interaction was detected. *$P<0.05$; **$P<0.01$; ***$P<0.001$ vs lean control ND; †$P<0.05$; ††$P<0.01$; †††$P<0.001$ vs obese control HFD. [a]$P<0.05$ effect of diet. [b]$P<0.05$ effect of surgery

Table 1 Metabolic profile following 4 weeks of surgical and dietary interventions in the different experimental groups of diet-induced obese rats

Determination	Lean—Control ND (n=22)	DIO—Sham ND (n=17)	DIO—Sleeve ND (n=15)	DIO—Pair-fed ND (n=17)	DIO—Control HFD (n=21)	DIO—Sham HFD (n=24)	DIO—Sleeve HFD (n=22)	DIO—Pair-fed HFD (n=23)	P diet	P surgery	P diet × surgery
Glucose (mg/dL)	80±2	80±3	77±3	94±4	90±2	94±4	96±3	103±5	0.001	0.001	0.081
Insulin (ng/mL)	2.1±0.4	1.0±0.2	1.1±0.3	1.4±0.1	3.6±0.6	3.0±0.4	2.3±0.2	3.3±0.3	0.067	0.070	0.196
HOMA	0.52±0.11	0.25±0.04	0.26±0.07	0.38±0.04	0.96±0.17	0.80±0.09	0.63±0.05	1.02±0.12	0.001	0.050	0.294
QUICKI	0.52±0.03	0.53±0.02	0.59±0.07	0.47±0.01	0.42±0.02	0.41±0.01	0.42±0.01	0.40±0.01	0.001	0.113	0.732
Glycerol (mg/dL)	29±3	27±1	26±2	28±2	33±3	25±2	22±2	27±2	0.008	0.010	0.963
FFA (mg/dL)	25±2	23±1	23±2	23±1	21±2	19±1	17±1	19±1	0.908	0.137	0.166
Adipo-IR index	258±48	132±15	126±20	194±23	400±85	320±35	212±15	393±64	0.001	0.009	0.451
TG (mg/dL)	142±28	88±7	59±6	73±7	100±11	89±9	67±7	87±10	0.002	0.001	0.796
Cholesterol (mg/dL)	105±7	104±4	103±5	105±3	115±8	106±5	94±6	107±7	0.007	0.111	0.021
Leptin (ng/mL)	7.7±1.1	6.7±0.9	5.6±0.9	8.6±0.7	17.1±1.4	11.3±1.2	9.0±1.0	15.0±1.0	0.001	0.001	0.054
Ghrelin (ng/mL)	0.93±0.10	1.03±0.10	0.54±0.07	1.10±0.10	0.71±0.07	0.94±0.08	0.50±0.03	1.00±0.10	0.014	0.000	0.898

Data are the mean±S.E.M. Statistical differences were analyzed by two-way ANOVA or one-way ANOVA followed by Tukey's *post hoc* test if an interaction was detected

DIO diet-induced obesity, *ND* normal diet, *HFD* high-fat diet, *HOMA* homeostasis model assessment, *QUICKI* quantitative insulin sensitivity check index, *FFA* free fatty acids, *TG* triacylglycerols

lower insulinemia (P=0.070), HOMA and adipo-IR indices (both P<0.05), as well as a better lipid profile, supported by lower (P<0.001) serum TG and total cholesterol. Interestingly, pair-fed groups neither improved glucose nor lipid metabolism. Changes in circulating concentrations of leptin and total ghrelin were analyzed as representative anorexigenic and orexigenic hormones, respectively. DIO rats exhibited lower (P<0.05) total ghrelin concentrations than the lean control group, with animals undergoing the sleeve gastrectomy showing a dramatic reduction (P<0.0001) in total ghrelin compared to sham-operated groups due to the resection of the gastric fundus. Serum leptin concentrations were increased (P<0.0001) in DIO rats compared to lean rats, while they decreased in the sleeve-gastrectomized animals compared to the other intervention groups.

Sleeve Gastrectomy is Associated with Opposite Changes in Both AQP3 and AQP7 Protein Levels when Comparing Epididymal and Subcutaneous Fat Depots

To analyze the potential involvement of aquaglyceroporins in the changes observed in adipose tissue hypertrophy after sleeve gastrectomy, we first assessed the gene and protein expression levels of AQP3 and AQP7 in paired samples of EWAT and SCWAT of the experimental groups by real-time PCR, Western blot, and immunohistochemistry (Figs. 2 and 3). As illustrated in Fig. 2a, b, tissue distribution of AQP3 and AQP7 showed a predominant immunostaining in the stromovascular fraction and lower expression in fully mature adipocytes, as previously described by our group and others [8, 35]. HFD feeding was associated with a modest increase in messenger RNA (mRNA) and protein expression of AQP3 without changes in AQP7 transcript and protein levels in EWAT compared to groups fed the ND (Fig. 2c–f). By contrast, SCWAT of DIO rats exhibited lower mRNA and protein expression of AQP3 and higher transcript and protein levels of AQP7 (Fig. 3a–d). Furthermore, *Aqp3* mRNA expression in EWAT was negatively correlated with markers of lipolysis, namely serum FFA (r=−0.41, P=0.0001) and glycerol (r=−0.26, P=0.004), while *Aqp7* transcript levels in EWAT and SCWAT were positively associated with the weight of each fat depot (r=0.25, P=0.005 and r=0.51, P<0.0001, respectively) as well as with glycemia (r=0.21, P=0.025 and r=0.29, P=0.002, respectively). Sleeve gastrectomy was associated with a downregulation (P<0.05) of the transcript and protein levels of AQP7 in EWAT and SCWAT in relation to sham-operated groups. By contrast, AQP3 protein levels were upregulated in EWAT after sleeve gastrectomy. No changes were observed in pair-fed animals, suggesting that changes in aquaglyceroporin expression in both fat depots are beyond food intake reduction.

It is well known that the expression of AQP7 is positively regulated by agonists of the master transcription factor of adipogenesis, PPARγ, in rodents [28, 36]. Thus, to gain further

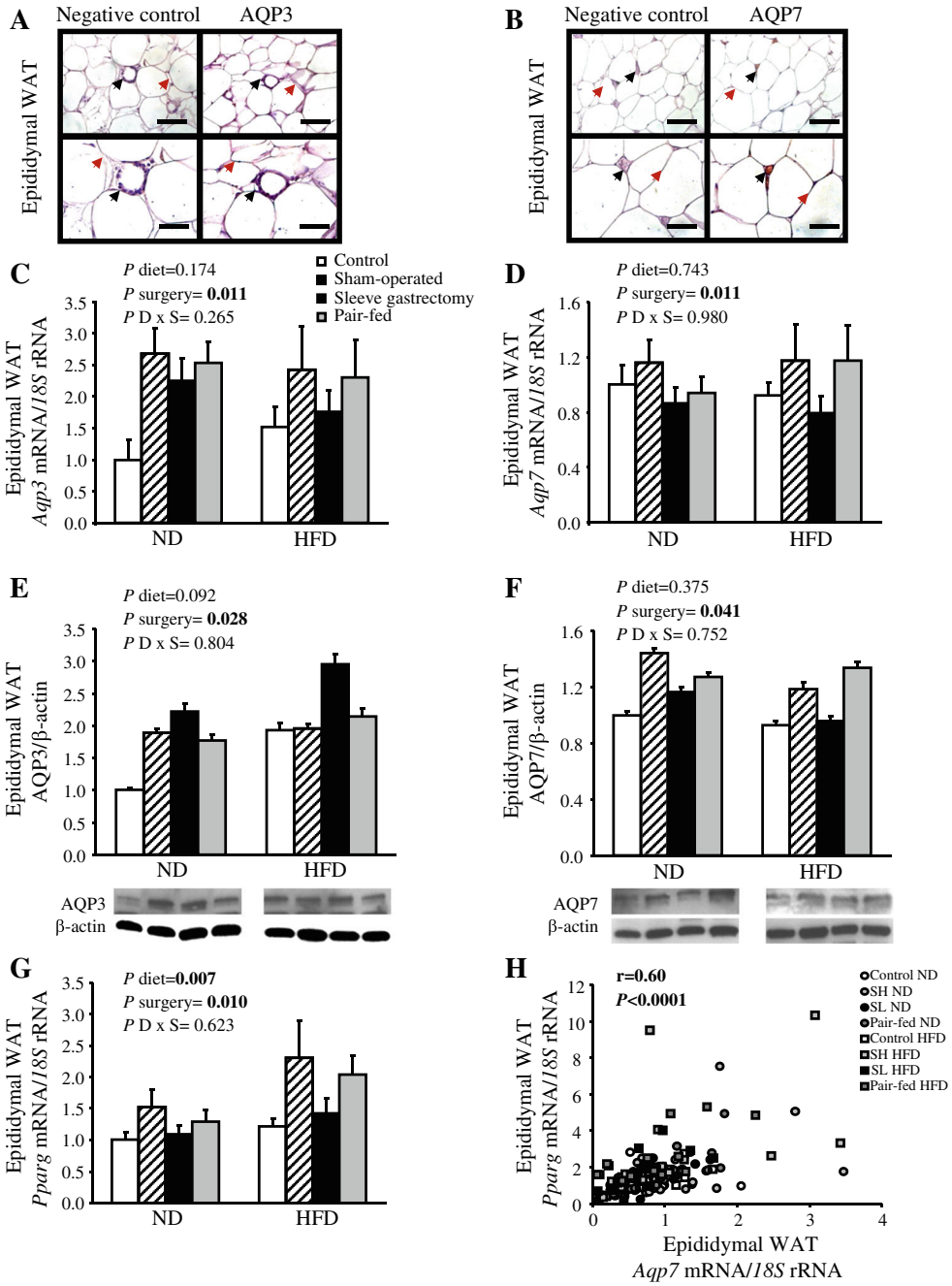

Fig. 2 Effect of sleeve gastrectomy on the expression of AQP3 and AQP7 in epididymal white adipose tissue (EWAT). Immunostaining of AQP3 (**a**) and AQP7 (**b**) in fully mature adipocytes (*red arrows*) and stromovascular fraction (*black arrows*) in rat EWAT (magnification 200×, *scale bar*= 100 μm in the *upper panels* and 400×, *scale bar*=50 μm in the *lower panels*). *Bar* graphs illustrate the gene and protein expression of AQP3 (**c**, **e**) and AQP7 (**d**, **f**) as well as *Pparg* transcript levels (**g**) in EWAT of the different experimental groups. Representative blots are shown at the bottom of the figure. (**h**) Scatter diagram showing the positive correlation between *Pparg* and *Aqp7* transcript levels in EWAT. The Pearson's correlation coefficient (*r*) and *P* values are indicated. The gene and protein expression in the control group fed a normal diet (ND) was assumed to be 1. Differences between groups were analyzed by two-way ANOVA

insight into the molecular mechanisms leading to the reduction of adiposity after sleeve gastrectomy, we analyzed the gene expression of *Pparg* in EWAT and SCWAT of the experimental animals. As expected, the transcript levels of *Pparg* were increased ($P<0.05$) in EWAT and SCWAT of DIO animals (Figs. 2g and 3e) and positively correlated with markers of adiposity, such as fat depot weight ($r=0.17$, $P=0.041$ and $r=0.28$, $P=0.035$, respectively) and serum leptin concentrations ($r=0.22$, $P=0.009$ and $r=0.23$, $P=0.008$, respectively). In line with these results, sleeve gastrectomy was associated with a reduction of *Pparg* mRNA levels in EWAT ($P<0.05$) and SCWAT, although changes in subcutaneous fat depot were not statistically significant ($P=0.293$). Caloric restriction by pair-feeding was also related to lower *Pparg* gene expression, but to a lesser extent than that observed after sleeve gastrectomy. It is also noteworthy that *Pparg* transcript levels were strongly associated with *Aqp7* in EWAT and SCWAT (both $P<0.0001$) (Figs. 2h and 3f).

Sleeve Gastrectomy Reduces Fatty Liver and Tends to Increase Hepatic AQP9 Expression

The rats fed a HFD showed an increase in liver weight ($P<0.0001$) and intrahepatic TG content ($P<0.0001$) as well

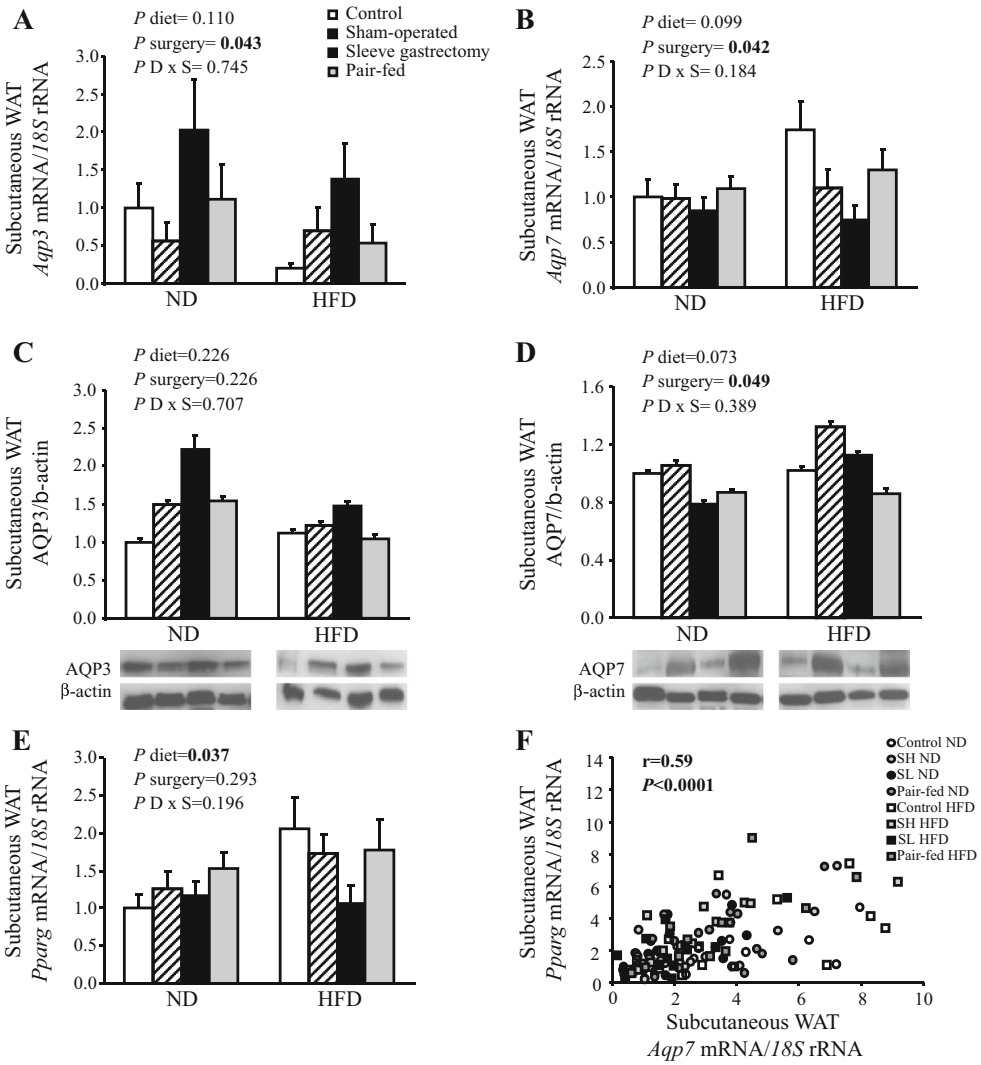

Fig. 3 Effect of sleeve gastrectomy on the expression of AQP3 and AQP7 in subcutaneous white adipose tissue (SCWAT). *Bar* graphs illustrate the gene and protein expression of AQP3 (**a**, **c**) and AQP7 (**b**, **d**) as well as *Pparg* transcript levels (**e**) in SCWAT of the different experimental groups. Representative blots are shown at the bottom of the figure. (**f**) Scatter diagram showing the positive correlation between *Pparg* and *Aqp7* transcript levels in SCWAT. The Pearson's correlation coefficient (*r*) and *P* values are indicated. The gene and protein expression in the control group fed a normal diet (ND) was assumed to be 1. Differences between groups were analyzed by two-way ANOVA

as macrovesicular steatosis (Fig. 4a–c). The switch to ND ($P<0.0001$) and surgical interventions ($P<0.05$) reduced the hepatic weight and steatosis, with rats undergoing sleeve gastrectomy displaying the highest reduction of liver weight and intrahepatic TG levels. Pair-feeding was associated with a lower reduction in intrahepatic TG than that observed in sleeve-gastrectomized rats, suggesting that the changes in liver steatosis after bariatric surgery are beyond caloric restriction. *Pparg* and *Srebf1* gene expression were also evaluated in liver samples as key signaling mechanisms associated with the onset of hepatic steatosis. Animals given the HFD showed an increase in *Pparg* ($P<0.05$) and *Srebf1* mRNA levels ($P<0.001$), whereas sleeve gastrectomy was associated with a downregulation of these lipogenic transcription factors, although only the reduction in *Pparg* mRNA was statistically significant ($P<0.05$) (Fig. 4d, e).

We next analyzed the expression of AQP9, the primary route for glycerol uptake in rat hepatocytes, by real-time PCR, Western blot, and immunohistochemistry. DIO was associated with a trend towards a lower expression of AQP9 mRNA and protein, with sleeve gastrectomy and caloric restriction increasing AQP9 gene and protein expression, but without reaching statistical significance (Fig. 5a, b). Liver sections showed a strong immunoreactivity for AQP9, which was mainly localized around the central veins (Fig. 5c). Interestingly, the *Aqp9* mRNA expression in liver was positively correlated with markers of lipolysis (FFA, $r=0.37$, $P=0.0001$) and insulin sensitivity (QUICKI, $r=0.18$, $P=0.047$), while they correlated negatively with markers of hepatic steatosis (intrahepatic TG, $r=-0.26$, $P=0.006$) and insulin resistance (insulin, $r=-0.23$, $P=0.009$; HOMA, $r=-0.18$, $P=0.045$). *Pparg* transcript levels were positively correlated with *Aqp9* in the liver (Fig. 5d).

Discussion

The prevalence of overweight and obesity in developed countries has increased markedly over the past three decades,

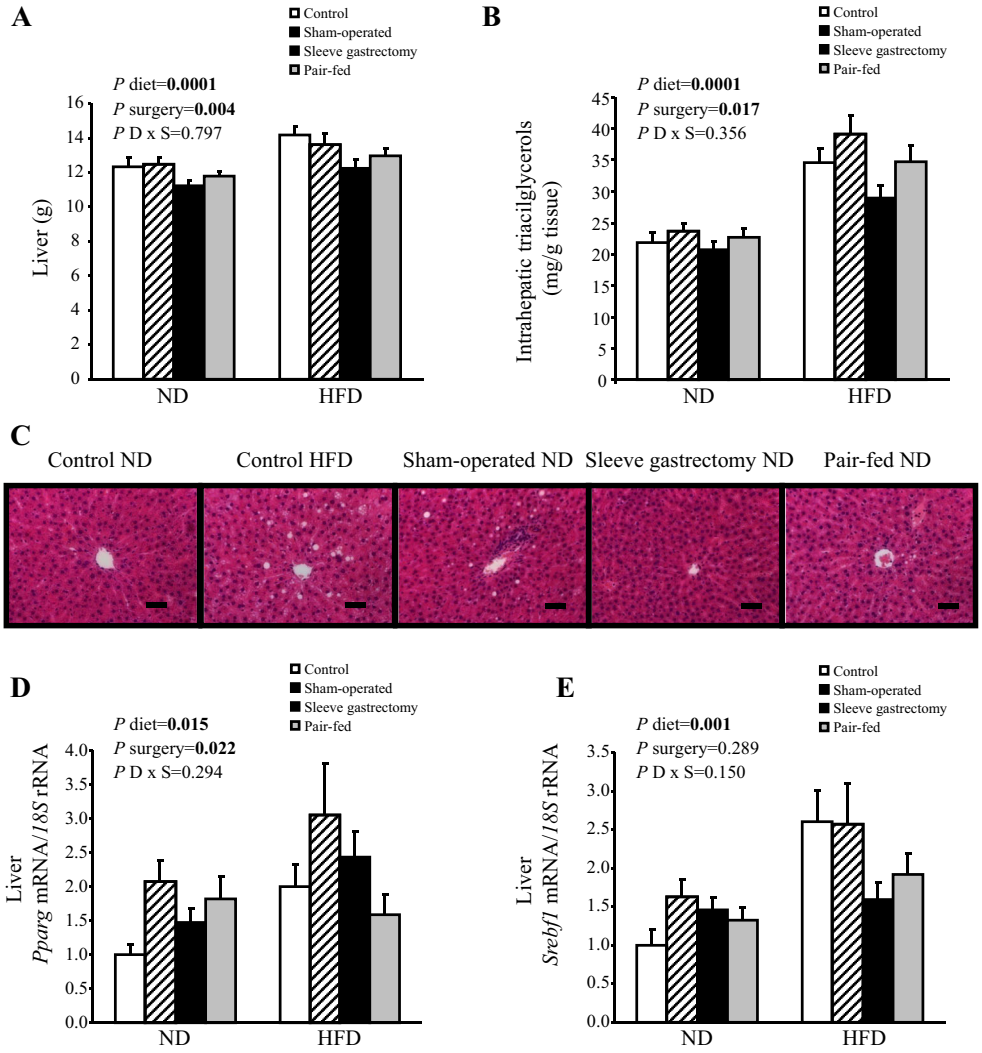

Fig. 4 Impact of sleeve gastrectomy on fatty liver in diet-induced obese animals. *Bar* graphs show the weight of the liver (**a**) as well as intrahepatic concentrations of triacylglycerols (**b**) of the animals after the surgical protocol (sham intervention or sleeve gastrectomy) and dietary interventions (normal diet [ND] vs high-fat diet [HFD] with ad libitum access or pair-fed to the amount of food eaten by sleeve-gastrectomized groups). (**c**) Representative images of liver sections of the experimental animals stained with hematoxylin-eosin are shown (magnification 200×, *scale bar*= 100 μm). *Bar* graphs show the gene expression levels of the lipogenic transcription factors *Pparg* (**d**) and *Srebf1* (**e**) in the liver of experimental groups. Differences between groups were analyzed by two-way ANOVA

becoming one of the leading causes of mortality worldwide [37]. Sleeve gastrectomy has emerged as an effective bariatric technique to induce weight loss in human morbid obesity [23] as well as in DIO rats [24, 25]. The present study shows that 4 weeks after surgery, rats undergoing sleeve gastrectomy showed lower body weight, whole-body adiposity as well as lower adipocyte hypertrophy. Moreover, sleeve gastrectomy improved insulin sensitivity and lipid profile, which is in agreement with several studies [38–40], including ours [26, 30, 41]. Our data support the hypothesis that the beneficial effects of sleeve gastrectomy go beyond food intake reduction, since the pair-fed groups exhibited higher body weight and adiposity than rats undergoing the sleeve gastrectomy. This bariatric procedure includes the resection of the gastric fundus, the major production site of ghrelin [42]. Accordingly, we found a dramatic reduction in circulating concentrations of the orexigenic hormone ghrelin in sleeve-gastrectomized animals even if fed a HFD, which may contribute to the higher weight loss when compared to pair-fed rats [30].

The molecular mechanisms whereby sleeve gastrectomy reduces adipocyte hypertrophy are not completely unraveled. In circumstances of negative energy balance, including caloric restriction or exercise, adipocytes hydrolyze TG into FFA and glycerol, which are released into the bloodstream [36]. AQP7, and to a lesser extent AQP3, constitute the major glycerol gateways in adipocytes [7, 8, 43]. AQP3 and AQP7 facilitate glycerol outflow from adipocytes in response to lipolysis induced by β-adrenergic agonists via its translocation from the cytosolic fraction (AQP3) or lipid droplets (AQP7) [8, 44, 45]. Our findings provide evidence that DIO was associated with a tendency towards an increase of AQP3 in EWAT and AQP7 in SCWAT, suggesting a higher lipolytic response in both fat depots. Moreover, ghrelin constitutes a negative regulator of AQP7 in adipocytes [27]. Thus, the higher gene expression levels of *Aqp7* found in DIO might be also related to the hypoghrelinemia of these animals. Our results show, for the first time, that sleeve gastrectomy results in an increase in EWAT AQP3, which may reflect a lipolytic rate improvement in this fat depot following this surgical intervention. By

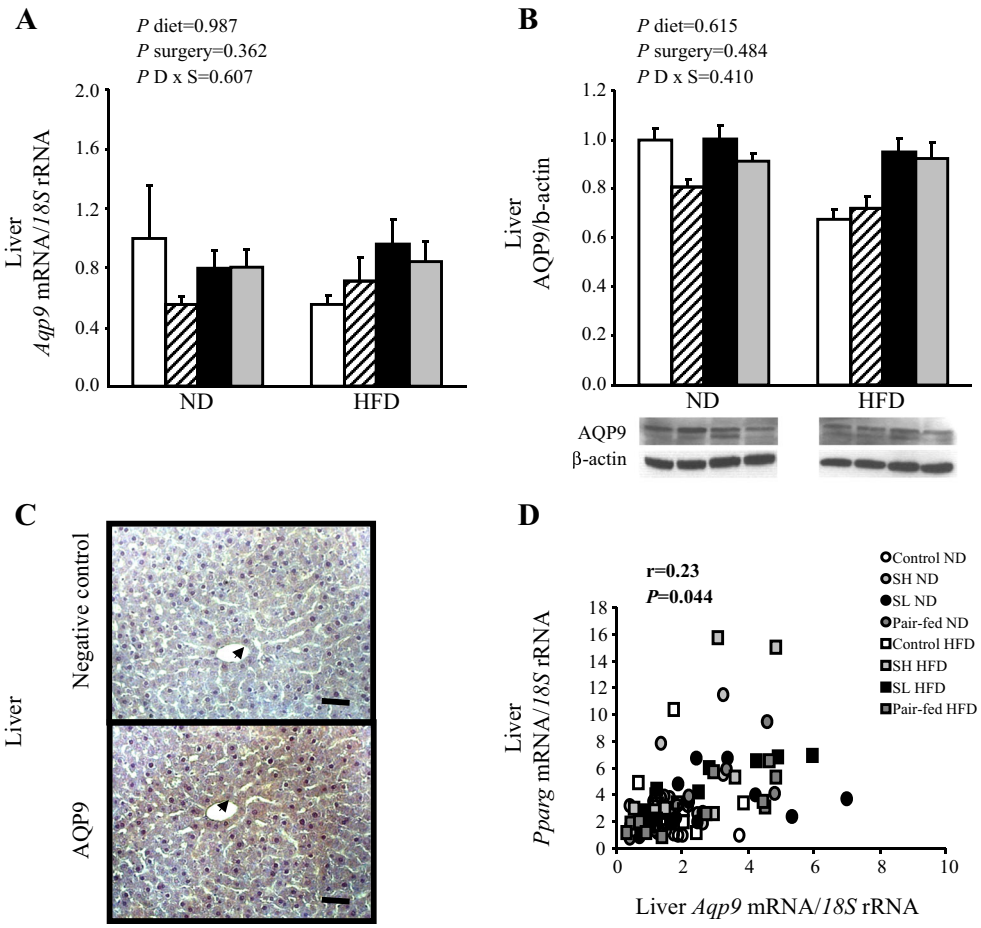

Fig. 5 Effect of sleeve gastrectomy on the hepatic expression of AQP9 of the different experimental groups. *Bar* graphs show the mRNA (**a**) and protein (**b**) expression levels of AQP9 in the liver of experimental animals after surgical and dietary interventions. The gene and protein expression in the control group fed a normal diet was assumed to be 1. Representative blots are shown at the bottom of the figure. Differences between groups were analyzed by two-way ANOVA. (**c**) Immunohistochemical detection of AQP9 protein (*black arrows*) in histological sections of rat liver (magnification 200×, *scale bar*=100 μm). (**d**) A positive correlation was found between hepatic *Pparg* and *Aqp9* transcript levels. The Pearson's correlation coefficient (*r*) and *P* values are indicated

contrast, the lower expression of AQP7 in both fat depots appears to be related to the reduction in the size of adipocytes after sleeve gastrectomy. Further studies are warranted in order to discern the differential regulation of aquaglyceroporins in adipose tissue after surgically induced weight loss.

Obesity is associated with an increased risk of NAFLD [46, 47]. Accordingly, in the present study, obese rats fed ad libitum a HFD exhibited higher hepatic steatosis than lean control rats. Several studies investigating the effect of bariatric surgery on NAFLD have shown an improvement in serum transaminases and hepatic histologic features after surgery [48, 49]. Our data showed that sleeve gastrectomy reduced DIO-induced intrahepatic TG accumulation and macrovesicular steatosis, which is in accordance with previous reports showing the beneficial effects of this bariatric procedure in the liver of experimental animals with genetic and DIO [50, 51]. The mechanisms underlying intrahepatic TG accumulation include excess dietary fat, increased delivery of FFA to the liver, inadequate FFA oxidation, and increased de novo lipogenesis [52]. In line with these observations, we found that DIO was associated with an increase in the gene expression levels of *Pparg* and *Srebf1*, two important lipogenic transcription factors. Sleeve gastrectomy reduced the transcript levels of PPARγ, suggesting the implication of this transcription factor in fatty liver improvement after surgery.

Hepatic TG synthesis requires both FFA and a source of glycerol-3-phosphate. During fasting, the source of glycerol-3-phosphate can either be plasma glucose via glycolysis or glycerol released from adipose tissue after lipolysis [5, 36, 53]. AQP9 constitutes the main gateway for glycerol uptake in hepatocytes [12, 14, 54]. AQP9 enables glycerol influx into hepatocytes, where it is converted to glycerol-3-phosphate by the enzymatic activity of GK and is used as a substrate for de novo synthesis of glucose and TG [54, 55]. Interestingly, our group has recently described that NAFLD is also associated with a downregulation of hepatic AQP9 in humans in parallel to the degree of steatosis [20]. This observation leads to the notion that lower intrahepatocellular glycerol due to a decreased AQP9 expression may represent a compensatory mechanism whereby the liver counteracts further TG accumulation within its parenchyma. Results reported herein showed that liver AQP9 immunostaining was mainly located around the portal vein, as earlier shown by our group and others [19, 20, 56, 57]. Consistent with previous studies [8, 18], lower mRNA and protein levels of AQP9 were found in DIO animals, although differences were not statistically significant. As expected, hepatic *Aqp9* expression was negatively

associated with markers of fatty liver, such as intrahepatic TG, and with insulin resistance, including insulinemia and the HOMA index. Interestingly, sleeve gastrectomy was associated with a slight increase in hepatic AQP9, which might reflect the recovery of glycerol uptake due to the improvement of hepatic steatosis and gluconeogenesis following weight loss.

The coordinated regulation of adipose and hepatic aquaglyceroporin expression is extremely relevant to maintain fat accumulation control and whole-body glucose homeostasis [8, 11]. We herein report, for the first time, that sleeve gastrectomy restores the coordinated regulation of fat-specific AQP7 and liver-specific AQP9, contributing to the prevention of excessive lipid accumulation in adipose tissue as well as the accumulation of TG in the liver parenchyma. Our results identify aquaglyceroporins as key elements in mediating part of the beneficial effects of bariatric surgery on NAFLD improvement via the regulation of glycerol availability, a key metabolite for hepatic TG synthesis. Further investigations in novel mutations, single-nucleotide polymorphisms or differential expression levels of aquaglyceroporins are required to establish the suitability of these glycerol pores as therapeutic targets for human obesity and obesity-associated fatty liver disease.

Acknowledgments We gratefully acknowledge the valuable collaboration of all the staff of the breeding house of the University of Navarra.

Conflict of Interest L.M.-G., S.B., R.M., V.V., B.R., A.L., J.G., I.B., J.A.C., V.C., S.F., J.G.-A., A.R., and G.F. declare that they have no conflict of interest.

Ethical Statement This article does not contain any studies with human participants.

Funding This work was supported by Fondo de Investigación Sanitaria-FEDER (FIS PI10/01677, PI12/00515, and PI13/01430) from the Spanish Instituto de Salud Carlos III, the Department of Health of the Gobierno de Navarra (61/2014) as well as by the Plan de Investigación de la Universidad de Navarra (project PIUNA 2011–14). CIBER de Fisiopatología de la Obesidad y Nutrición (CIBERobn) is an initiative of the Instituto de Salud Carlos III, Spain.

References

1. King LS, Kozono D, Agre P. From structure to disease: the evolving tale of aquaporin biology. Nat Rev Mol Cell Biol. 2004;5:687–98.
2. Verkman AS, Anderson MO, Papadopoulos MC. Aquaporins: important but elusive drug targets. Nat Rev Drug Discov. 2014;13:259–77.
3. Frühbeck G. Obesity: aquaporin enters the picture. Nature. 2005;438:436–7.
4. Rodríguez A, Catalán V, Gómez-Ambrosi J, Frühbeck G. Aquaglyceroporins serve as metabolic gateways in adiposity and insulin resistance control. Cell Cycle. 2011;10:1548–56.
5. Reshef L, Olswang Y, Cassuto H, Blum B, Croniger CM, Kalhan SC, et al. Glyceroneogenesis and the triglyceride/fatty acid cycle. J Biol Chem. 2003;278:30413–6.
6. Hibuse T, Maeda N, Funahashi T, Yamamoto K, Nagasawa A, Mizunoya W, et al. Aquaporin 7 deficiency is associated with development of obesity through activation of adipose glycerol kinase. Proc Natl Acad Sci U S A. 2005;102:10993–8.
7. Hara-Chikuma M, Sohara E, Rai T, Ikawa M, Okabe M, Sasaki S, et al. Progressive adipocyte hypertrophy in aquaporin-7-deficient mice: adipocyte glycerol permeability as a novel regulator of fat accumulation. J Biol Chem. 2005;280:15493–6.
8. Rodríguez A, Catalán V, Gómez-Ambrosi J, García-Navarro S, Rotellar F, Valentí V, et al. Insulin- and leptin-mediated control of aquaglyceroporins in human adipocytes and hepatocytes is mediated via the PI3K/Akt/mTOR signaling cascade. J Clin Endocrinol Metab. 2011;96:E586–97.
9. Laforenza U, Scaffino MF, Gastaldi G. Aquaporin-10 represents an alternative pathway for glycerol efflux from human adipocytes. PLoS One. 2013;8:e54474.
10. Madeira A, Fernandez-Veledo S, Camps M, Zorzano A, Moura TF, Ceperuelo-Mallafré V, et al. Human aquaporin-11 is a water and glycerol channel and localizes in the vicinity of lipid droplets in human adipocytes. Obesity (Silver Spring). 2014;22:2010–7.
11. Kuriyama H, Shimomura I, Kishida K, Kondo H, Furuyama N, Nishizawa H, et al. Coordinated regulation of fat-specific and liver-specific glycerol channels, aquaporin adipose and aquaporin 9. Diabetes. 2002;51:2915–21.
12. Rojek AM, Skowronski MT, Fuchtbauer EM, Fuchtbauer AC, Fenton RA, Agre P, et al. Defective glycerol metabolism in aquaporin 9 (AQP9) knockout mice. Proc Natl Acad Sci U S A. 2007;104:3609–14.
13. Ma T, Song Y, Yang B, Gillespie A, Carlson EJ, Epstein CJ, et al. Nephrogenic diabetes insipidus in mice lacking aquaporin-3 water channels. Proc Natl Acad Sci U S A. 2000;97:4386–91.
14. Calamita G, Gena P, Ferri D, Rosito A, Rojek A, Nielsen S, et al. Biophysical assessment of aquaporin-9 as principal facilitative pathway in mouse liver import of glucogenetic glycerol. Biol Cell. 2012;104:342–51.
15. Morinaga T, Nakakoshi M, Hirao A, Imai M, Ishibashi K. Mouse aquaporin 10 gene (AQP10) is a pseudogene. Biochem Biophys Res Commun. 2002;294:630–4.
16. Marrades MP, Milagro FI, Martínez JA, Moreno-Aliaga MJ. Differential expression of aquaporin 7 in adipose tissue of lean and obese high fat consumers. Biochem Biophys Res Commun. 2006;339:785–9.
17. Prudente S, Flex E, Morini E, Turchi F, Capponi D, De Cosmo S, et al. A functional variant of the adipocyte glycerol channel aquaporin 7 gene is associated with obesity and related metabolic abnormalities. Diabetes. 2007;56:1468–74.
18. Catalán V, Gómez-Ambrosi J, Pastor C, Rotellar F, Silva C, Rodríguez A, et al. Influence of morbid obesity and insulin resistance on gene expression levels of AQP7 in visceral adipose tissue and AQP9 in liver. Obes Surg. 2008;18:695–701.
19. Gena P, Mastrodonato M, Portincasa P, Fanelli E, Mentino D, Rodríguez A, et al. Liver glycerol permeability and aquaporin-9 are dysregulated in a murine model of non-alcoholic fatty liver disease. PLoS One. 2013;8:e78139.
20. Rodríguez A, Gena P, Méndez-Giménez L, Rosito A, Valentí V, Rotellar F, et al. Reduced hepatic aquaporin-9 and glycerol permeability are related to insulin resistance in non-alcoholic fatty liver disease. Int J Obes. 2014;38:1213–20.
21. Wang C, Lv ZL, Kang YJ, Xiang TX, Wang PL, Jiang Z. Aquaporin-9 downregulation prevents steatosis in oleic acid-induced non-alcoholic fatty liver disease cell models. Int J Mol Med. 2013;32:1159–65.
22. Deitel M, Crosby RD, Gagner M. The first international consensus summit for sleeve gastrectomy (SG), New York City, October 25-27, 2007. Obes Surg. 2008;18:487–96.
23. Gagner M, Deitel M, Erickson AL, Crosby RD. Survey on laparoscopic sleeve gastrectomy (LSG) at the Fourth International

Consensus Summit on Sleeve Gastrectomy. Obes Surg. 2013;23: 2013–7.
24. de Bona CJ, Bettiol J, d'Acampora AJ, Castelan JV, de Souza JC, Bressiani V, et al. Sleeve gastrectomy model in Wistar rats. Obes Surg. 2007;17:957–61.
25. Valentí V, Martín M, Ramírez B, Gómez-Ambrosi J, Rodríguez A, Catalán V, et al. Sleeve gastrectomy induces weight loss in diet-induced obese rats even if high-fat feeding is continued. Obes Surg. 2011;21:1438–43.
26. Rodríguez A, Becerril S, Valentí V, Ramírez B, Martín M, Méndez-Giménez L, et al. Sleeve gastrectomy reduces blood pressure in obese (*fa*/*fa*) Zucker rats. Obes Surg. 2012;22:309–15.
27. Rodríguez A, Gómez-Ambrosi J, Catalán V, Gil MJ, Becerril S, Sáinz N, et al. Acylated and desacyl ghrelin stimulate lipid accumulation in human visceral adipocytes. Int J Obes. 2009;33:541–52.
28. Kishida K, Shimomura I, Nishizawa H, Maeda N, Kuriyama H, Kondo H, et al. Enhancement of the aquaporin adipose gene expression by a peroxisome proliferator-activated receptor γ. J Biol Chem. 2001;276:48572–9.
29. Frühbeck G, Alonso R, Marzo F, Santidrián S. A modified method for the indirect quantitative analysis of phytate in foodstuffs. Anal Biochem. 1995;225:206–12.
30. Rodríguez A, Becerril S, Valentí V, Moncada R, Méndez-Giménez L, Ramírez B, et al. Short-term effects of sleeve gastrectomy and caloric restriction on blood pressure in diet-induced obese rats. Obes Surg. 2012;22:1481–90.
31. Muruzabal FJ, Frühbeck G, Gómez-Ambrosi J, Archanco M, Burrell MA. Immunocytochemical detection of leptin in non-mammalian vertebrate stomach. Gen Comp Endocrinol. 2002;128:149–52.
32. Frühbeck G, Gómez-Ambrosi J, Salvador J. Leptin-induced lipolysis opposes the tonic inhibition of endogenous adenosine in white adipocytes. FASEB J. 2001;15:333–40.
33. Catalán V, Gómez-Ambrosi J, Rotellar F, Silva C, Gil MJ, Rodríguez A, et al. The obestatin receptor (GPR39) is expressed in human adipose tissue and is down-regulated in obesity-associated type 2 diabetes mellitus. Clin Endocrinol (Oxf). 2007;66:598–601.
34. Becerril S, Rodríguez A, Catalán V, Sainz N, Ramírez B, Collantes M, et al. Deletion of inducible nitric-oxide synthase in leptin-deficient mice improves brown adipose tissue function. PLoS One. 2010;5: e10962.
35. Skowronski MT, Lebeck J, Rojek A, Praetorius J, Fuchtbauer EM, Frokiaer J, et al. AQP7 is localized in capillaries of adipose tissue, cardiac and striated muscle: implications in glycerol metabolism. Am J Physiol Renal Physiol. 2007;292:F956–65.
36. Méndez-Giménez L, Rodríguez A, Balaguer I, Frühbeck G. Role of aquaglyceroporins and caveolins in energy and metabolic homeostasis. Mol Cell Endocrinol. 2014. doi:10.1016/j.mce.2014.06.017.
37. Frühbeck G, Toplak H, Woodward E, Yumuk V, Maislos M, Oppert JM. Executive Committee of the European Association for the Study of Obesity. Obesity: the gateway to ill health—an EASO position statement on a rising public health, clinical and scientific challenge in Europe. Obes Facts. 2013;6:117–20.
38. Wilson-Perez HE, Chambers AP, Sandoval DA, Stefater MA, Woods SC, Benoit SC, et al. The effect of vertical sleeve gastrectomy on food choice in rats. Int J Obes. 2013;37:288–95.
39. Patrikakos P, Toutouzas KG, Perrea D, Menenakos E, Pantopoulou A, Thomopoulos T, et al. A surgical rat model of sleeve gastrectomy with staple technique: long-term weight loss results. Obes Surg. 2009;19:1586–90.
40. Stefater MA, Perez-Tilve D, Chambers AP, Wilson-Perez HE, Sandoval DA, Berger J, et al. Sleeve gastrectomy induces loss of weight and fat mass in obese rats, but does not affect leptin sensitivity. Gastroenterology. 2010;138:2426–36. 36 e1-3.
41. Lancha A, Moncada R, Valentí V, Rodríguez A, Catalán V, Becerril S, et al. Effect of sleeve gastrectomy on osteopontin circulating levels and expression in adipose tissue and liver in rats. Obes Surg. 2014;24: 1702–8.
42. Frühbeck G, Díez Caballero A, Gil MJ. Fundus functionality and ghrelin concentrations after bariatric surgery. N Engl J Med. 2004;350:308–9.
43. Madeira A, Camps M, Zorzano A, Moura TF, Soveral G. Biophysical assessment of human aquaporin-7 as a water and glycerol channel in 3T3-L1 adipocytes. PLoS One. 2013;8:e83442.
44. Kishida K, Kuriyama H, Funahashi T, Shimomura I, Kihara S, Ouchi N, et al. Aquaporin adipose, a putative glycerol channel in adipocytes. J Biol Chem. 2000;275:20896–902.
45. Yasui H, Kubota M, Iguchi K, Usui S, Kiho T, Hirano K. Membrane trafficking of aquaporin 3 induced by epinephrine. Biochem Biophys Res Commun. 2008;373:613–7.
46. Chalasani N, Younossi Z, Lavine JE, Diehl AM, Brunt EM, Cusi K, et al. The diagnosis and management of non-alcoholic fatty liver disease: Practice Guideline by the American Gastroenterological Association, American Association for the Study of Liver Diseases, and the American College of Gastroenterology. Gastroenterology. 2012;142:1592–609.
47. Clark JM. The epidemiology of nonalcoholic fatty liver disease in adults. J Clin Gastroenterol. 2006;40 Suppl 1:S5–10.
48. Dixon JB, Bhathal PS, O'Brien PE. Weight loss and non-alcoholic fatty liver disease: falls in gamma-glutamyl transferase concentrations are associated with histologic improvement. Obes Surg. 2006;16:1278–86.
49. Burza MA, Romeo S, Kotronen A, Svensson PA, Sjoholm K, Torgerson JS, et al. Long-term effect of bariatric surgery on liver enzymes in the Swedish obese subjects (SOS) study. PLoS One. 2013;8:e60495.
50. Wang Y, Liu J. Sleeve gastrectomy relieves steatohepatitis in high-fat-diet-induced obese rats. Obes Surg. 2009;19:921–5.
51. Kawano Y, Ohta M, Hirashita T, Masuda T, Inomata M, Kitano S. Effects of sleeve gastrectomy on lipid metabolism in an obese diabetic rat model. Obes Surg. 2013;23:1947–56.
52. Utzschneider KM, Kahn SE. Review: the role of insulin resistance in nonalcoholic fatty liver disease. J Clin Endocrinol Metab. 2006;91: 4753–61.
53. Kalhan SC, Mahajan S, Burkett E, Reshef L, Hanson RW. Glyceroneogenesis and the source of glycerol for hepatic triacylglycerol synthesis in humans. J Biol Chem. 2001;276:12928–31.
54. Jelen S, Wacker S, Aponte-Santamaria C, Skott M, Rojek A, Johanson U, et al. Aquaporin-9 protein is the primary route of hepatocyte glycerol uptake for glycerol gluconeogenesis in mice. J Biol Chem. 2011;286:44319–25.
55. Lebeck J. Metabolic impact of the glycerol channels AQP7 and AQP9 in adipose tissue and liver. J Mol Endocrinol. 2014;52: R165–78.
56. Elkjaer M, Vajda Z, Nejsum LN, Kwon T, Jensen UB, Amiry-Moghaddam M, et al. Immunolocalization of AQP9 in liver, epididymis, testis, spleen, and brain. Biochem Biophys Res Commun. 2000;276:1118–28.
57. Nicchia GP, Frigeri A, Nico B, Ribatti D, Svelto M. Tissue distribution and membrane localization of aquaporin-9 water channel: evidence for sex-linked differences in liver. J Histochem Cytochem. 2001;49:1547–56.